Appl Nanosci (2014) 4:477–484
DOI 10.1007/s13204-013-0221-1

ORIGINAL ARTICLE

Conjunctive effect of CMC–zero-valent iron nanoparticles and FYM in the remediation of chromium-contaminated soils

Vemula Madhavi · Tollamadugu Naga Venkata Krishna Vara Prasad · Balam Ravindra Reddy · Ambavaram Vijay Bhaskar Reddy · Madhavi Gajulapalle

Received: 28 March 2013 / Accepted: 1 April 2013 / Published online: 19 April 2013

Abstract Chromium is an important industrial metal used in various products and processes but at the same time causing lethal environmental hazards. Remediation of Cr-contaminated soils poses both technological and economic challenges, as conventional methods are often too expensive and difficult to operate. Zero-valent iron particles at nanoscale are proposed to be one of the important reductants of Cr(VI), transforming the same into nontoxic Cr(III). In the present investigation, soils contaminated with Cr(VI) are allowed to react with the various loadings of zero-valent iron nanoparticles (Fe^0) for a reaction period of 24 h. Fe^0 nanoparticles were synthesized by the reduction of ferrous sulfate in the presence of sodium borohydride and stabilized with carboxy methyl cellulose and were characterized by scanning electron microscopy, energy dispersion spectroscopy, X-ray diffraction, UV–vis spectrophotometer, Fourier transform-infra red spectrophotometer, Raman spectroscopy, dynamic light scattering technique and zeta potential. Further, this work demonstrates the potential utilization of farm yard manure (FYM) and Fe^0 nanoparticles in combination and individually for the effective remediation of Cr(VI)-contaminated soils. An increase in the reduction of Cr(VI) from 60 to 80 % was recorded with the increase in the loading of Fe^0 nanoparticles from 0.1 to 0.3 mg/100 g individually and in combination with FYM ranging from 50 to 100 mg/100 g soil.

Keywords Chromium · Farm yard manure · Nanoparticles · Remediation · Zero-valent iron · Zeta potential

Introduction

Chromium which falls in the heavy metal category has been known for its toxicity since a century or more (Barceloux and Barceloux 1999). According to its toxicity, Cr was classified as a primary pollutant and ranked as second among many toxic metals in the environment for frequency of occurrence at Department of Energy (DOE) sites (Sparks 1995). WHO-allowed maximum concentration of Cr(VI) in drinking water is 0.05 mg/l. Chromium compounds are used in various industries (e.g. textile dying, tanneries, metallurgy, metal electroplating, electronic, and wood preserving); hence, large quantities of Cr have been discharged into the environment due to improper disposal and leakage (Kimbrough et al. 1999). Cr exists primarily in two-valence states, i.e., trivalent Cr(III) and hexavalent Cr(VI). Cr(VI) is highly toxic, soluble, and mobile in the aquatic systems (Cheryl and Susan 2008). Moreover, Cr(VI) has been classified as a potential carcinogen, mutagen, and teratogen and has acute toxicity for different biological systems. Cr(III), on the other hand, is less toxic, immobile, and readily precipitates as $Cr(OH)_3$ under alkaline or even slightly acidic conditions (Puls et al. 1999). Cr(III) is also an important micronutrient in the biological activity of insulin, is relatively stable and has low solubility in aqueous solution. The compounds of

Electronic supplementary material The online version of this article (doi:10.1007/s13204-013-0221-1) contains supplementary material, which is available to authorized users.

V. Madhavi · A. V. B. Reddy · M. Gajulapalle (✉)
Department of Chemistry, Sri Venkateswara University, Tirupati, AP, India
e-mail: gmkr555@yahoo.co.in

T. N. V. K. V. Prasad · B. R. Reddy
S.V.Agricultural College, Acharya N G Ranga Agricultural University, Tirupati 517 502, India

Cr(III) are reported to be 10–100 times less toxic than those of Cr(VI) (Wei et al. 1993).

Several techniques for Cr(VI) removal such as ion exchange, filtration, electrochemical precipitation, activated carbon adsorption, bioremediation, etc., have been reported in literature. However, these conventional methods are relatively expensive and complicated. Ionic state of the reductant plays an important role in remediation of the heavy metals. In this context, zero-valent iron (Fe^0) nanoparticle technology offers a potential advantage over conventional methods because of its unique physico-chemical properties, enhanced surface energy, non-toxicity and economical viability. Fe^0 nanoparticles have long been used in the electronic and chemical industries due to their magnetic and catalytic properties. Nowadays, use of Fe^0 nanoparticles is becoming an increasingly popular method for treatment of hazardous and toxic wastes and for remediation of contaminated soil and ground water (Li and Zhang 2006; Lien et al. 2006). Fe^0 nanoparticles provide a high surface-to-volume ratio, which promotes mass transfer to and from the solid surface resulting in high potential for contaminant removal and degradation (Martin et al. 2008). Mixing Fe^0 and sand (yielding Fe^0/sand filters) at suitable proportions has been proposed as a promising option for safe drinking water production (Chicgoua Noubactep et al. 2010). Diminutive size and large specific surface area of Fe^0 nanoparticles translate to enhanced reactivity for contaminant remediation. Generally, because of size effects and much surface free-energy, nanoparticles in aqueous media tend to aggregate rapidly (Yang et al. 2007) or react quickly with the surrounding media such as dissolved oxygen or water, resulting in much larger chains and loss of reactivity and transfer in contaminated sites. Therefore, it is important to increase the stability and transportability of nanoparticles into the subsoil and groundwater. In this case, various particle-stabilizing agents have been employed, including resin and starch (He and Zhao 2005), chitosan and carboxymethyl cellulose (Geng et al. 2009).

Suitable conditions for Cr(VI) reduction occur where organic matter is present and Cr(VI) reduction is enhanced in acidic rather than alkaline soils (Bartlett and Kimble 1976). Various organic materials, such as powdered leaves (Suseela et al. 1987) and Scotch pine (*Pinus sylvestris* L.) bark (Alves et al. 1993) have been used to remove Cr(VI) from industrial effluents. The natural organic matter (NOM) such as humic acid with Fe^0 nanoparticles plays an important role in Cr(VI) reduction by adsorption phenomena (Singh et al. 2011). Hence, in the present study it is proposed to use Fe^0 nanoparticles synthesized by using borohydride as reducing agents of ferrous ions and CMC as stabilizing agent and were tested for their potential in the remediation of Cr(VI)-contaminated soils individually and in combination with the farm yard manure (FYM).

Materials and methods

Chemicals and solutions

Ferrous sulfate heptahydrate ($FeSO_4 \cdot 7H_2O$) and sodium borohydride ($NaBH_4$) were purchased from Merck, India. 1,5-Diphenylcarbazide ($C_{13}H_{14}N_4O$) was procured from SD Fine Chemicals Ltd., India, carboxy methyl cellulose (CMC) and ethanol (C_2H_5OH) obtained from Merck, India, were used without any dilution.

Collection of soil samples

Soil sample was collected from the CL leather industry, Vellore, Tamilnadu following US EPA standard operating procedures for soil sampling (US EPA 2000) in the month of September 2012. After collection, all the samples were air dried, passed through a 2 mm sieve, packed in plastic bags and then stored in dark at 4 °C. Estimation of the heavy metals concentration in soil samples in triplicate was carried out using ICP-OES technique.

Synthesis of Fe^0 nanoparticles

The CMC-stabilized Fe^0 nanoparticles were freshly synthesized by following the methods reported by Wei et al. (2004) and He and Zhao (2005). In brief, the iron nanoparticles were synthesized by adding stoichiometric amounts of $NaBH_4$ in 30 % ethanol solution at a BH_4^-/Fe^{2+} molar ratio of 2.0 dropwise to a 1,000 mL three-necked flask containing $FeSO_4 \cdot 7H_2O$ aqueous solution and CMC with electrical stirring at ambient temperature. Before use, deionized water and the CMC solution were purged with purified N_2 to remove dissolved oxygen.

Characterization of Fe^0 nanoparticles

Fe^0 nanoparticles as prepared were characterized using multiple techniques like SEM, EDS, UV–vis, FT-IR, Raman spectroscopy, dynamic light scattering (DLS) for particle size determination and zeta potential.

SEM and EDS

Morphological studies of as prepared CMC-stabilized Fe^0 nanoparticles were carried out by using scanning electron microscope (SEM) fitted with an energy dispersive spectrophotometer (EDS) system (model CARL-ZEISS EVO MA 15). The sample was observed at 10,000× magnification

with an accelerating voltage of 20 kV. The energy dispersive spectrograph reveals strong signal in the iron region and confirms the formation of iron nanoparticles.

UV–vis spectroscopy

The localized surface plasmon resonance (LSPR) of Fe^0 nanoparticles stabilized with the CMC was recorded using Shimadzu UV 2450 UV–vis spectrophotometer and their absorption maxima at 300 nm which is a characteristic of monodispersed iron nanoparticles observed.

FTIR spectroscopy

The FTIR spectra of the CMC-stabilized Fe^0 nanoparticles were recorded in the transmission mode at room temperature using KBr pellet technique (1:20). The KBr was dried in a dryer at 200 °C for 24 h, then 560 mg KBr was homogenized with sample and afterwards ground to fine powder with a mortar and pestle. FTIR-Tensor 27(Bruker) infrared spectrophotometer was used to determine the spectra of the sample which was mixed with spectrally pure KBr and pressed to form thin plates (radius 1 cm, thickness 0.1 cm), then subjected to IR spectroscopic analysis in the spectral range 500 and 4,000 cm^{-1}.

X-ray diffraction

The method of X-ray diffraction (XRD) was used to investigate the material structure of iron nanoparticles. The XRD analysis was conducted with a Philips XRD 3100 diffractometer (Philips electronics Co.,) at 45 kV and 30 mA. It used copper Kα radiation and a graphite monochromator to produce X-rays with a wavelength of 1.54 Å. Iron nanoparticles were placed in a glass holder and scanned from 20° to 90°. This scan range covered all major species of iron and iron oxides. The scanning rate was set at 2.0°/min.

Zeta potential and particle size determination

The particle size and particle distribution width by DLS were obtained by using SZ-100 nanoparticle, a flexible analytical tool for characterizing the physical properties of small particles. The configuration and application of the system can be used as a particle size analyzer and also to measure zeta potential. Zeta potential was taken under the temperature of 25 °C; the dispersion medium has the viscosity 0.893 mPa and the electrode voltage at 3.4 V.

Raman spectroscopy

Raman spectroscopy allows characterization of many types of samples without any specific preparation. The Raman spectra were obtained using a Lab RAM HR visible single spectrometer equipped with a microscope and a Peltier-cooled CCD detector. The 633 nm He–Ne laser line was used for excitation. Raman measurements were performed at room temperature and atmospheric pressure. The characteristic peak positions of iron-based particles were determined in the Raman region of interest in this investigation: 100–1,200 cm^{-1}. The most intense peak positions for Raman spectra present in our sample for Fe^0 are at 223.6, 291.2 cm^{-1}.

Colorimetric method for analysis of Cr(VI)

Method 7196 A-USEPA was followed for the analysis of Cr(VI) in the present study. For this, 1,5-diphenyl carbazide solution was prepared by dissolving 250 mg diphenylcarbazide in 50 mL acetone. 1.0 mL of the extract to be tested was transferred to 10.0 mL volumetric flask. 200 µL of diphenylcarbazide solution was added to it and mixed properly. Then five drops of 1 N HNO_3 was added to maintain its pH = 2 ± 0.5. The volume was made up to 10 mL with distilled water and allowed to stand for 5–10 min for full color development. For quantification, an appropriate portion of it was transferred to cuvette and the absorbance at 540 nm was measured on spectrophotometer. Cr(VI) was analyzed in three systems, i.e., blank solution, stock solution and sample solutions. It was established that absorbance is linearly dependent on the metal concentration;

Table 1 Heavy metals present in the soil samples determined by ICP-OES

Element	Metal conc. in (ppm)
As	0.524 ± 0.05
B	0.362 ± 0.08
Ca	36.080 ± 2.5
Cd	0.111 ± 0.01
Cr	8.514 ± 1.6
Cu	0.731 ± 0.09
Fe	117.119 ± 5.3
Hg	0.352 ± 0.09
K	9.206 ± 1.2
Mg	20.022 ± 1.8
Mn	0.932 ± 0.1
Mo	0.421 ± 0.07
Na	12.532 ± 1.20
P	0.813 ± 0.14
Pb	0.940 ± 0.20
Se	0.551 ± 0.07
Ni	0.505 ± 0.04
Zn	1.493 ± 0.12

The values presented in the table are ±SE of three replicates

all the systems were run in parallel, in triplicates under similar experimental conditions. Heavy metals present in sample were determined by digesting the sample with 10 mL of digestion mixture ([HNO_3] + [HCl] in 3:1 ratio) in 250-mL conical flasks. The mixture was heated at 90–95 °C till the completion of digestion. It was then filtered and transferred into a 100-mL volumetric flask. Finally, the volume was made up to the mark with 1 % HNO_3. The samples were then analyzed on ICP-OES. Cr(III) was estimated by subtracting Cr(VI) from total Cr (Table 1).

Effect of Fe^0 concentration

Experiments were carried out to determine the concentration at which maximum reduction of Cr(VI) occurs. Various concentrations ranging from 0.1 to 0.3 mg of CMC–Fe^0 nanoparticles were added to 100 g of Cr(VI)-contaminated soil. After that the reaction mixture was extracted and analyzed for Cr(VI).

Effect of organic amendment (farm yard manure) on removal efficiency of Cr(VI) by Fe^0 nanoparticles

To investigate the effect of organic amendment (FYM) on removal efficiency of Cr(VI) by Fe^0 nanoparticles, two different concentrations (50, 100 mg) of FYM was spiked in 100 g of Cr(VI)-contaminated soil samples. These samples were treated with 0.1, 0.2, 0.3 mg of Fe^0 nanoparticles. After that the reaction mixture was extracted and analyzed for Cr(VI).

Results and discussion

The ferrous iron was reduced to zero-valent iron according to the following reaction:

$$4Fe^{2+}(aq) + 3BH_4^- + 9H_2O \rightarrow 4Fe^0(S) \downarrow + 3H_2BO_3 + 12H^+(aq) + 6H_2(g) \uparrow \quad (1)$$

The formed Fe^0 nanoparticles were observed to be highly stable for longer period when compared to unstabilized Fe^0. The UV–vis spectrum of Fe^0 nanoparticles in CMC is shown in (Fig. 1a). The Fe^0 nanoparticles showed their absorption maxima at 300 nm. CMC alone did not show any peak. This observation is similar to that obtained by Morgada et al. (2009). FTIR techniques provide information about vibrational state of adsorbed molecule and hence the nature of surface complexes. The band at 3,347 cm^{-1} was ascribed to OH stretching vibration and the one at 1,636 cm^{-1} to the OH bending vibration of surface-adsorbed water (Fig. 1b) which suggests the formation of ferric oxyhydroxide (FeOOH) layer on Fe^0 nanoparticles. The EDS and Raman spectrum (Fig. 1c, d) reveal strong signal in the iron region and confirm the formation of iron nanoparticles. SEM image (Fig. 2) of Fe^0 nanoparticles showed that the nanoparticles are mostly spherical in shape forming chain like aggregates. After the examination of more than 200 nanoparticles, a particle size distribution was calculated, which indicates that 90 % of the particles were within the range of 100 nm, although few large aggregates with diameter around 200 nm were also observed. The average size found was 70.2 nm and standard deviation

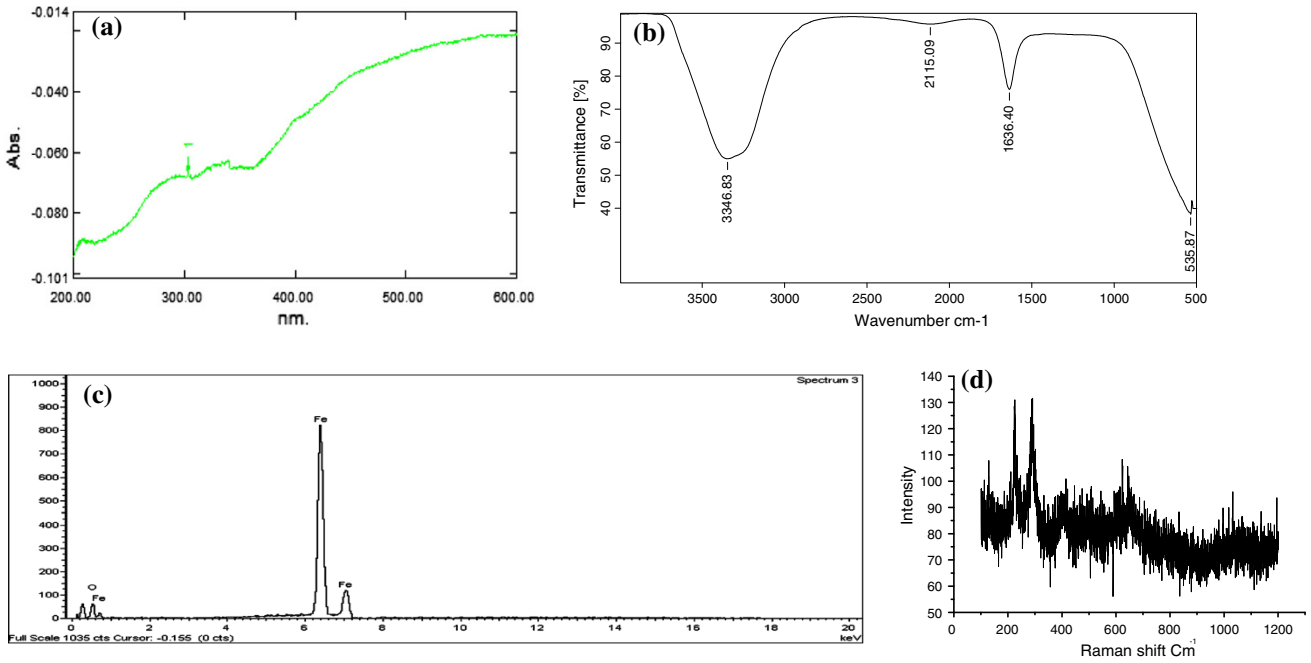

Fig. 1 Spectra of CMC-stabilized Fe^0 nanoparticles: **a** UV–vis, **b** FT-IR, **c** EDS and **d** Raman spectroscopy

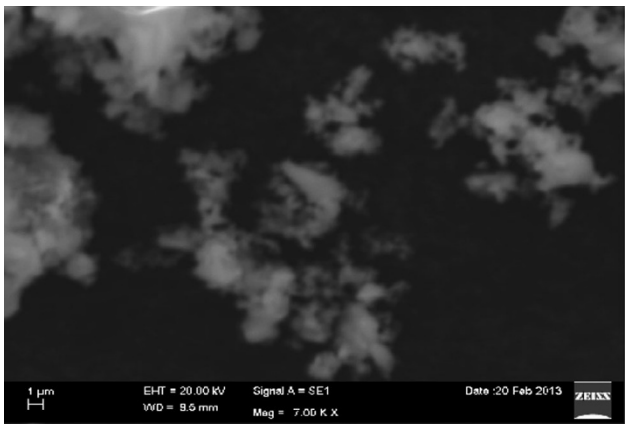

Fig. 2 SEM of CMC-stabilized Fe^0 nanoparticles

62.9 nm. Particles size was further determined by using DLS. The mean hydrodynamic diameter was found to be 74.5 nm, approximately the same size which was determined with SEM. The XRD analysis of Fe^0 nanoparticles is shown in Fig. 3. The peak at 2 h of 44.751° indicates the presence of Fe^0 nanoparticles. Zeta potential measurements (Fig. 4) were largely consistent with particle size distribution data and indicated the stability of the suspensions. The magnitude of the zeta potential gives an indication of the potential stability of the colloidal system. If all the particles in suspension have a large negative or positive zeta potential then they will tend to repel each other and there will be no tendency for the particles to come together. The zeta potential of Fe^0 nanoparticles synthesized is −60.8 mV. Particles with zeta potentials more positive than +30 mV or more negative than −30 mV are normally considered stable. A comparative remediation study was carried out using three concentrations of CMC-stabilized Fe^0 nanoparticles ranging from 0.1 to 0.3 mg/100 g in order to evaluate the redox performance for reduction of Cr(VI) for 24 h. Results showed the increase in the reduction of Cr(VI) with the increase in concentration of Fe^0 nanoparticles. It is believed that the Cr(VI) reductive reaction occurs on the Fe^0 nanoparticle surfaces. As the Fe^0 nanoparticles mass concentration increases, the reactive Fe sites increase proportionally, which lead to the increase of Cr(VI) removal efficiency. Effect of FYM on removal efficiency of Cr(VI) by Fe^0 nanoparticles is illustrated in Fig. 5. The data showed the increase in the Cr(VI) reduction with the increase in FYM concentration in 1 day. These observations indicate that the reduction of Cr by Fe^0 nanoparticle is based on the transformation of Cr(VI) to Cr(III). These observations are in agreement with the observations of Powell et al. (1995) and Powell and Puls (1997), who had given a thorough evaluation of the Cr(VI) removal by Fe^0 in systems of natural aquifer materials with varying geochemistry and suggested that the mechanism of Cr(VI) reduction by Fe^0 is a cyclic, multiple reaction electrochemical corrosion mechanism.

It is desirable that the reduction of Cr(VI) present in soil is accompanied by immobilization in soil of the corresponding insoluble reduced chromium species. The efficiency presented by ZVI for the remediation of soil containing Cr(VI) can be evaluated comparing the different findings. As expected the analysis of findings obtained for ZVI with increased FYM revealed that S1N3F2 presented a higher efficiency for reduction of Cr(VI) (81 %) when compared to the other treatments.

Li and Zhang (2007) explained the reduction of metal cations on the basis of the standard electrode potential (E^0) of the metal ions. For the metals having E^0 greatly positive than E^0 of Fe^0 such as Cu^{2+}, Hg^{2+}, and Ag^+, predominant removal mechanism is reduction. Removal via sorption and reductive precipitation is followed by metals having E^0 slightly more positive than that of Fe^0 (Pb^{2+}, Ni^{2+}) and the metals having E^0 more negative than Fe^0, such as Zn^{2+} and Cd^{2+} removed by sorption or surface complexation procedure. The standard electrode potentials of Fe^0, Cr(VI), and Cr(III) are −0.41, 1.36, and −0.74 V, respectively. Spectroscopic data have also shown that Cr $(OH)_3$ and

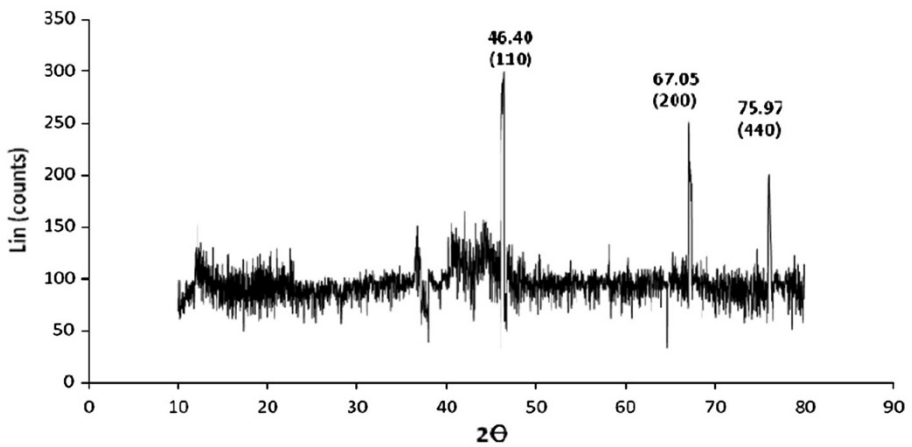

Fig. 3 XRD pattern of CMC-stabilized Fe^0 nanoparticles

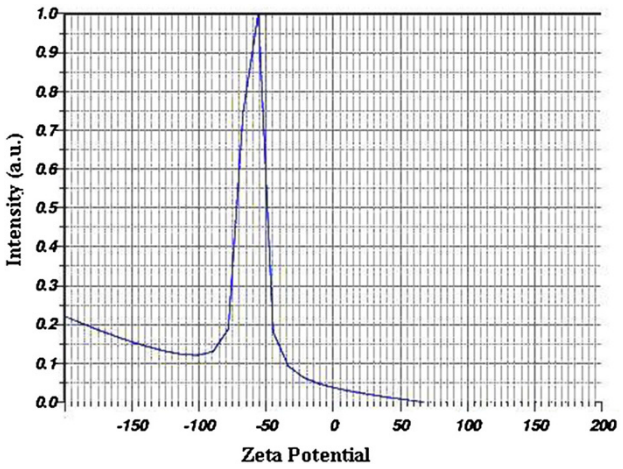

Fig. 4 Zeta potential of CMC-stabilized Fe^0 nanoparticles

mixed Cr(III)/Fe(III) hydroxides are precipitated on the iron surface (Powell et al. 1995; Pratt et al. 1997; Ponder et al. 2000). The net reactions of Cr(VI) reduction with Fe^0 and the co-precipitation of Cr(III) and Fe(III) could be expressed by Eqs. (2) and (3). No dissolved Cr(III) was detected during the reaction, which suggests that all the Cr(III) was co-precipitated with Fe(III). This observation is consistent with those reported previously (Williams and Scherer 2001; He and Trainas 2005). It can be concluded that iron hydroxide and chromium hydroxide could be the final and predominant products of Cr(VI) reduction by CMC-stabilized Fe^0 nanoparticles.

$$CrO_4^{2-} + Fe^0 + 8H^+ \rightarrow Fe^{3+} + Cr^{3+} + 4H_2O \quad (2)$$

$$(1-x)Fe^{3+} + xCr^{3+} + 2H_2O \rightarrow Fe_{(1-x)}Cr_xOOH \downarrow +3H^+ \quad (3)$$

On the basis of solution chemistry and X-ray photoelectron spectroscopy data, Li et al. (2008) determined the average value of x, and it was found to be approximately 0.667. This Cr–Fe oxyhydroxide shell is stable and serves as a sink for Cr(VI). Fe^0 nanoparticles exhibit characteristics of both iron oxyhydroxides (i.e., as a sorbent) and metallic iron (i.e., as reductant). For Cr(VI) removal, Fe^0 nanoparticles mainly act as a reductant. The chemical reduction of Cr(VI) to Cr(III) is accompanied by chromium immobilization in soil via formation of an insoluble mixed oxide compound (Débora Franco et al. 2009). The reduced Cr(III) can be incorporated into the iron oxyhydroxide shell forming $(Cr_xFe_{1-x})(OH)_3$ or $Cr_xFe_{(1-x)}OOH$ at the surface. At high initial Cr concentration, this structure may serve as a passive layer at the surface and hinder further reduction of Cr(VI). After reduction, Cr(III) may be removed through the precipitation or co-precipitation in terms of $(Cr_xFe_{1-x})(OH)_3$ or $Cr_xFe_{(1-x)}OOH$ as its E^0 is (−0.74 V) which is slightly more than E^0 of Fe^0 nanoparticle.

Addition of biological waste materials such as FYM has often been shown to increase the amount of dissolved organic carbon (DOC) in soils either by acting as a source of DOC or by enhancing the solubilization of the soil organic matter (Schindler et al. 1992). The FYM plays an important role in Cr(VI) reduction by virtue of functional groups such as hydroquinones. The hydroquinone groups of DOC were identified as the major source of electron donor for the reduction of Cr(VI) to Cr(III) in soils (Elovitz and Fish 1995):

$$3CH_2O(\text{organic matter}) + 2Cr_2O_7^{-2} + 16H^+ \rightarrow 4Cr^{3+} + 16H^+3CO_2 + 11H_2O \quad (4)$$

The statistical results for the above experiment revealed that there is a consistency in results.

The experimental procedure and the results were analyzed statistically using SAS 9.3. The general linear model fitted to the data and the model is highly significant even at 1 % level of significance with R^2 0.95. The absorbance comparison for sample treatments analysis revealed that, there is highly significant difference in absorption of control, i.e., bulk iron treatment (S1B1) with Fe^0 nanoparticles individually and also in combination with FYM (Fig. 6). The significance of pair wise differences (<0.01) on absorption in different treatments was also recorded. The

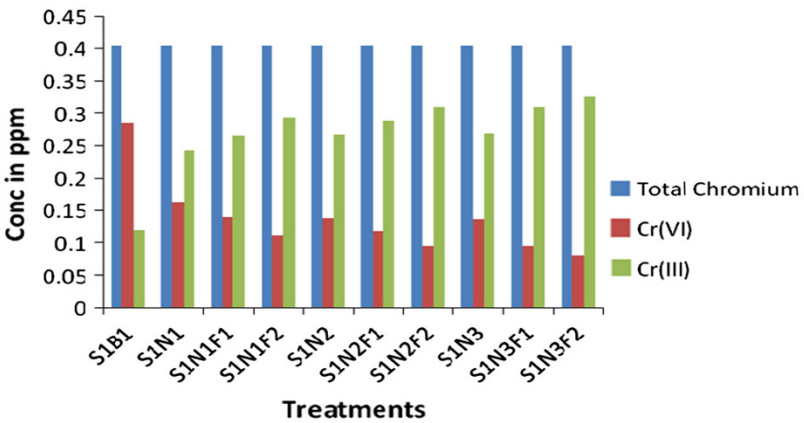

Fig. 5 Effect of Fe^0 nanoparticles with and without FYM on Cr(VI) reduction, initial Cr(VI) concentration in surface soil (S_1) = 0.4032 ppm, Fe^0 conc. (bulk) B_1 = 0.1 mg/100 g, Fe^0 conc. (nano) N_1 = 0.1, N_2 = 0.2, N_3 = 0.3 mg/100 g, F1 = FYM (50 mg/100 g), F2 = FYM (100 mg/100 g), time = 24 h

box plot (Fig. 7) for absorption within replications shows the consistency of the experiment.

Our speculation is that the FYM with Fe^0 nanoparticle-assisted reduction of Cr(VI) in this study may be explained as per the earlier citations by the researchers. The organic amendment which is rich in ammoniacal N oxidizes to nitrate NO_3^- resulted in the release of protons (Bolan et al. 2003). This may be one of the reasons for the decrease of soil pH that can inhibit the iron corrosion thereby prolonging the life time of nano Fe^0. On the other hand the FYM can also transfer electrons from Fe^0 to reduce Cr(VI) in the soil. Hence, the reduction of Cr(VI) increased in the presence of FYM-assisted Fe^0 nanoparticles than unassisted nano Fe^0 particles. This is supported by earlier studies which have shown that the reduction of Cr(VI) to Cr(III) with Fe^0 nanoparticles was found to increase with the decrease in soil pH. (Debora Franco et al. 2009).

Further, Paul and Beauchamp(1989) reported that the easily oxidisable organic carbon and DOC fractions provide the energy source for microorganisms involved in the reduction of metals such as, Cr[i.e., Cr(VI) to Cr(III)]. Hence the DOC, ammoniacal nitrogen and microorganisms in organic amendments influence the performance of Fe^0 nanoparticles. Several authors reported the chromium detoxification by microorganisms by various processes such as biotransformation, bioremediation and biosorption. The carbonyl, hydroxyl, sulphydryl, amino and phosphate groups on the microorganisms play a vital role in reduction of Cr(VI) (Chand et al. 1994). On the basis of above studies, it may be concluded that the FYM used in the present study may have high microbial activity and also assists Fe^0 nanoparticles in Cr(VI) reduction. Further studies in this direction will help to elucidate the detailed mechanism of the role of microbial activity in Fe^0 nanoparticle-mediated reactions.

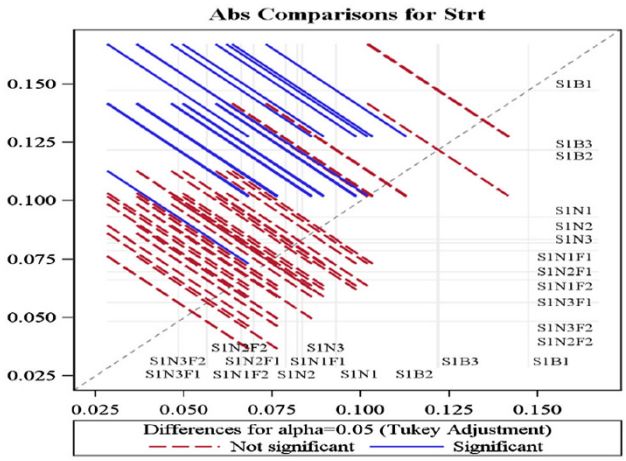

Fig. 6 Absorption comparisons for soil treatments

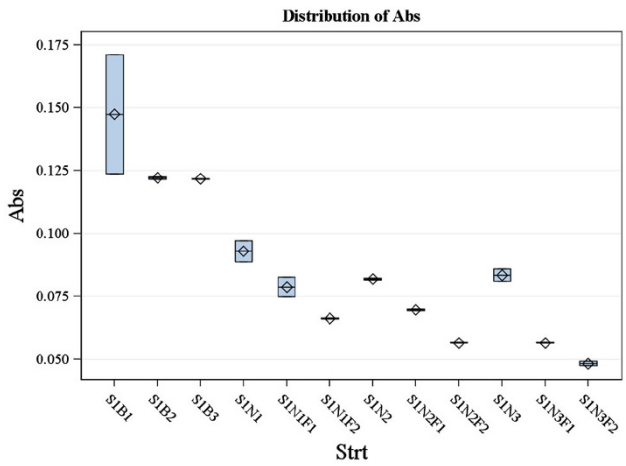

Fig. 7 The box plot for absorption within replications

Conclusions

CMC-stabilized Fe^0 nanoparticles were synthesized and were used to reduce Cr(VI). The CMC-stabilized Fe^0 nanoparticles exhibited higher removal efficiency than those prepared without a stabilizer because the CMC acted as a good dispersant to prevent Fe^0 nanoparticles from agglomerating. Addition of FYM to Fe^0 nanoparticles facilitates the effective reduction of Cr(VI) concentration. The study further suggests that the stabilized Fe^0 nanoparticles may be used for in situ reductive immobilization of Cr(VI)-contaminated soils or other Cr(VI)-laden solid wastes, which may lead to an innovative remediation technology that is likely more cost-effective and less environmentally disruptive.

Acknowledgments The authors are thankful to Department of Physics, SV University for providing the data on Raman spectroscopy.

References

Alves M, Gonzalez BCG, De Carvalho GR, Castenheira JM, Pereira SMC, Vasconcelos LAT (1993) Chromium removal in tannery wastewaters—Polishing by *Pinus sylvestris* bark. Water Res 27:1333–1338

Barceloux DG, Barceloux D (1999) Chromium. Clinical Toxicology 37(2):173–194

Bartlett RJ, Kimble JM (1976) Behavior of chromium in soils: II. Hexavalent forms. J Environ Qual 5:383–386

Bolan NS, Adriano DC, Natesan R, Koo B-J (2003) Effects of organic amendments on the reduction and phytoavailability of chromate in mineral soil. J Environ Qual 32:120–128

Chand S, Agrawal VK, Kumar P (1994) Removal of hexavalent chromium from waste water by adsorption. Indian J Environ Health 36(3):151–158

Cheryl P, Susan MB (2008) Reflections on hexavalent chromium: health hazards of an industrial heavyweight. Environ Health Perspect 108:48–58

Debora Franco V, Leonardo Da Silva M, Wilson Jardim F (2009) Chemical reduction of hexavalent chromium present in contaminated soil using a packed-bed column reactor. Clean 37(11):858–865

Débora Franco V, Leonardo Da Silva M, Wilson Jardim F (2009) Reduction of hexavalent chromium in soil and ground water using zero-valent iron under batch and semi-batch conditions. Water Air Soil Pollut 197:49–60

Elovitz MS, Fish W (1995) Redox interactions of Cr(VI) and substituted phenols: products and mechanisms. Environ Sci Technol 29:1933–1943

Geng B, Jin Z, Li T, Oi X (2009) Preparation of chitosan-stabilized Fe 0 nanoparticles for removal of hexavalent chromium in water. Sci Total Environ 407:4994–5000

He YT, Trainas SJ (2005) Cr(VI) reduction and immobilization by magnetite under alkaline pH conditions: the role of passivation. Environ Sci Technol 39:4499–4504

He F, Zhao D (2005) Preparation and characterization of a new class of starch-stabilized bimetallic nanoparticles for degradation of chlorinated hydrocarbons in water. Environ Sci Technol 39:3314–3320

Kimbrough DE, Cohen Y, Winer AM, Creelman L, Mabuni C (1999) Critical assessment of chromium in the environment. Crit Rev Environ Sci Techno 29:1–46

Li XQ, Zhang WX (2006) Iron nanoparticles: the core-shell structure and unique properties for Ni (II) sequestration. Langmuir 22:4638–4642

Li XQ, Zhang WX (2007) Sequestration of metal cations with zerovalent iron nanoparticles—A study with high resolution X ray photoelectron spectroscopy (HRXPS). J Phys Chem C 111:699–6946

Li XQ, Cao J, Zhang WX (2008) Stoichiometry of Cr(VI) immobilization using nanoscale zerovalent iron (nZVI): a study with high-resolution X-ray photoelectron spectroscopy (HR-XPS). Ind Eng Chem Res 47:2131–2139

Lien HI, Elliott DW, San YP, Zhang WX (2006) Recent progress in zero-valent iron nanoparticles for groundwater remediation. J Environ Eng Manag 16:371–380

Martin JE, Herzing AA, Yan W, Li XQ, Koel BE, Kieley CJ, Zhang WX (2008) Determination of the oxide layer thickness in core-shell zerovalent iron nanoparticles. Langmuir 24:4329–4334

Morgada ME, Levy IK, Salomone V, Farias SS, Lopez G, Litter MI (2009) Arsenic (V) removal with nanoparticulate zerovalent iron: effect of UV light and humic acids. Catal Today 143:261–268

Noubactep C, Care S, Togue-Kamga F, Schöner A, Woafo P (2010) Extending service life of household water filters by mixing metallic iron with sand. Clean–Soil Air Water 38(10):951–959

Paul JW, Beauchamp EG (1989) Effect of carbon constituents in manure on denitrification in soil. Can J Soil Sci 69:49–61

Ponder SM, Darab JG, Mallouk TE (2000) Remediation of Cr(VI) and Pb(II) aqueous solutions using supported, nano-scale zero valent iron. Environ Sci Technol 34:2564–2569

Powell RM, Puls RW (1997) Proton generation by dissolution of intrinsic or augmented aluminosilicate minerals for in situ contaminant remediation by zero valence-state iron. Environ Sci Technol 31:2244–2251

Powell RM, Puls RW, Hightower SK, Sabatini DA (1995) Coupled iron corrosion and chromate reduction: mechanism of subsurface remediation. Environ Sci Technol 29:1913–1922

Pratt AR, Blowes DW, Ptacek CJ (1997) Products of chromate reduction on proposed subsurface remediation material. Environ Sci Technol 31:2492–2498

Puls RW, Paul CJ, Powell RM (1999) The application of in situ permeable reactive (Zero-valent iron) barrier technology for the remediation of chromate contaminated ground water: a field test. Appl Geochem 14:989–1000

Schindler DW, Bayley SE, Curtis PJ, Parker BR, Stainton MP, Kelly CA (1992) Natural and man-caused factors affecting the abundance and cycling of dissolved organic substances in Precambrian shield lakes. Hydrobiologia 229:1–21

Singh R, Misra V, Singh RP (2011) Synthesis, characterization and role of zero-valent iron nanoparticle in removal of hexavalent chromium from chromium-spiked soil. J Nanopart Res 13:4063–4073

Sparks DL (1995) Environmental soil chemistry. Academic Press, San Diego

Suseela K, Sivaparvathi M, Nandy SC (1987) Removal of chromium from tannery effluent using powdered leaves. Leather Sci. (Madras) 34:149–156

U.S. EPA Environmental Response Team (2000) Standard Operating Procedures SOP-2012, Soil sampling, pp 1–13

Wei C, German S, Basak S, Rajeshwar K (1993) Reduction of hexavalent chromium in aqueous solutions by polypyrrole. J Electrochem Soc 140:60–62

Wei JJ, Xu XH, Liu Y (2004) Kinetics and mechanism of dechlorination of o-chlorophenol by nanoscale Pd/Fe. Chem Res Chin Univ 20:73–76

Williams AGB, Scherer MM (2001) Kinetics of Cr(VI) reduction by carbonate green rust. Environ Sci Technol 35:3488–3494

Yang GCC, Tu HC, Hung CH (2007) Stability of nanoiron slurries and their transport in the subsurface environment. Sep Purif Technol 58:166–172